Improved spectral representations of neutron-star equations of state

Lee Lindblom

Center for Astrophysics and Space Sciences, University of California at San Diego, La Jolla, California 92093, USA

(Received 24 February 2022; accepted 17 March 2022; published 31 March 2022)

Spectral representations have been shown to provide an efficient way to represent the poorly understood high-density portion of the neutron-star equation of state. This paper shows how the efficiency and accuracy of those representations can be improved by a very simple change.

DOI: 10.1103/PhysRevD.105.063031

I. INTRODUCTION

Spectral representations have been shown to be accurate and efficient ways to parametrize the high-density portions of the neutron-star equation of state [1,2]. Consequently these representations are being used by several groups now to extract equation of state information from data obtained by x-ray and gravitational-wave observations of neutron stars, see e.g., Refs. [3–5]. This paper shows how a very simple change can increase the accuracy and efficiency of these spectral representations.

Spectral representations of the equation of state are smooth (assuming smooth spectral basis functions are used), while the highest density portion of the real neutron-star equation of state may have nonsmooth points that arise from physical phase transitions. However, spectral representations are efficient ways to represent even nonsmooth functions, e.g. Fourier series can even be used to represent discontinuous functions. Spectral representations of the high-density neutron-star equation of state have been tested and shown to be reasonably accurate for some theoretical model equations of state that contain phase transitions in [1,2]. However, the accuracy of a spectral representation in the neighborhood of any nonsmooth point is reduced, and the convergence rate of its average error is slower (typically power law instead of exponential) when nonsmooth points are present. The purpose of this paper is to propose a way to increase the smoothness of the spectral model equations of state at the point where they match onto the low-density equation of state, and to test how this change effects the accuracy of those representations.

Section II briefly reviews and then shows how to improve the basic pressure-based representations constructed from spectral expansions of the adiabatic index of the material, see Ref. [1]. Section III reviews and then shows how to improve the pressure-based causal representations constructed from spectral expansions related to the sound speed of the material, see Ref. [2]. Finally, Sec. IV shows how these improvements can be extended to the enthalpy-based representations of the equations of state, which are useful for some purposes [6]. The accuracy and efficiency of the improved spectral representations in each section are evaluated by computing and then testing best-fit representations of 27 realistic theoretical neutron-star equations of state.

II. BASIC SPECTRAL REPRESENTATIONS

Previous studies [1,2] have shown that efficient and accurate representations of neutron-star equations of state can be constructed using spectral representations of key thermodynamic quantities. The first of these were based on spectral expansions of the adiabatic index $\Gamma(p)$, defined by

$$\Gamma(p) = \frac{\epsilon(p) + p}{p} \left(\frac{d\epsilon}{dp} \right)^{-1}. \tag{1}$$

These basic spectral expansions have the form

$$\Gamma(p) = \exp\left[\sum_k \gamma_k \Phi_k(p) \right], \tag{2}$$

where the $\Phi_k(p)$ are a suitable fixed set of spectral basis functions, and the γ_k are the spectral coefficients that determine a particular $\Gamma(p)$ in this representation.

As shown in [1], any adiabatic index $\Gamma(p)$ on the domain $p \geq p_0$ determines the equation of state $\epsilon(p)$ on that domain:

$$\epsilon(p) = \frac{\epsilon_0}{\mu(p)} + \frac{1}{\mu(p)} \int_{p_0}^{p} \frac{\mu(p')}{\Gamma(p')} dp', \tag{3}$$

where $\mu(p)$ is defined by

$$\mu(p) = \exp\left[- \int_{p_0}^{p} \frac{dp'}{p' \Gamma(p')} \right]. \tag{4}$$

The spectral coefficients γ_k determine the adiabatic index from Eq. (2), and then Eqs. (3) and (4) together with the

integration constants ϵ_0 and p_0 uniquely determine the equation of state in these basic pressure-based spectral representations.

The constants ϵ_0 and p_0 are the pressure and density at the point where the spectral representation matches onto a low-density equation of state: $\epsilon(p_0) = \epsilon_0$. These constants, ϵ_0 and p_0, ensure that the match between the low-density equation of state and the high-density spectral expansion is continuous. However, they do not ensure that the derivative of the equation of state is continuous at this point. The presence of a discontinuity in the derivative would indicate, implicitly, the presence of a phase transition in the material. The matching point is typically chosen at sufficiently low density that no physical phase transition should be present there. Additional constraints on the spectral representation would be needed to ensure that no such unphysical discontinuity occurs there.

The spectral basis functions used in the basic spectral expansions introduced in [1] have the form,

$$\Phi_k(p) = \left[\log\left(\frac{p}{p_0}\right)\right]^k. \tag{5}$$

In the basic spectral expansions $\Gamma(p_0) = \exp(\gamma_0)$ since $\Phi_0(p_0) = 1$ and $\Phi_k(p_0) = 0$ for $k > 0$. It follows that the continuity at the matching point of $\Gamma(p)$, and hence the derivative of the equation of state, is determined completely by the lowest-order spectral coefficient γ_0. This continuity is assured if and only if γ_0 is chosen to be $\gamma_0 = \log\Gamma_0$, where Γ_0 is determined from the low-density equation of state:

$$\Gamma_0 = \frac{\epsilon_0 + p_0}{p_0}\left(\left.\frac{d\epsilon(p)}{dp}\right|_{p\uparrow p_0}\right)^{-1}. \tag{6}$$

In [1] the accuracy and efficiency of these spectral representations were tested by adjusting the n lowest spectral coefficients $\{\gamma_0, \gamma_1, \ldots, \gamma_{n-1}\}$ to provided the best-fit representations of realistic equation of state models in the density range relevant for neutron stars. For finite n the spectral representations do not necessarily satisfy the derivative continuity condition, $\Gamma(p_0) = \exp(\gamma_0) = \Gamma_0$, exactly. (Although in the limit of large n this discontinuity becomes arbitrarily small in these representations.) Figure 1 illustrates the slope discontinuities at the matching point for the lowest-order basic spectral fits of the APR1 equation of state.[1]

The unphysical discontinuities in the derivatives of the equations of state at the point (p_0, ϵ_0) can, however, be removed simply by changing the way the best-fit spectral coefficients are determined. Instead of adjusting the

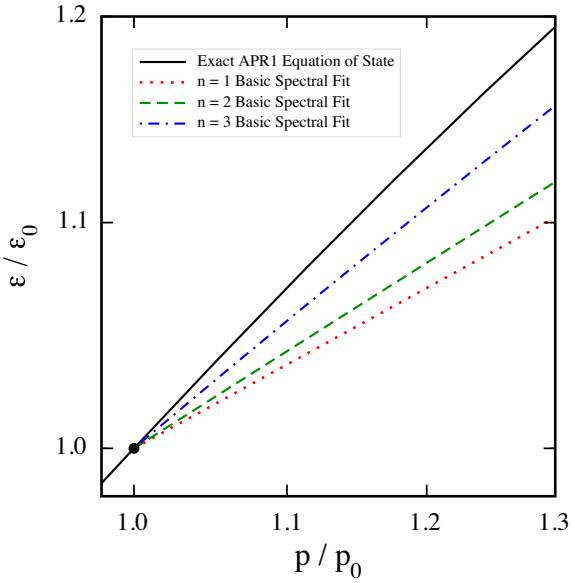

FIG. 1. Discontinuities in the slopes of the best-fit basic pressure-based spectral representations of the equation of state are illustrated at the point (p_0, ϵ_0) (black dot) where they match onto the low-density equation of state. The exact equation of state shown here as the solid (black) curve is the APR1 equation of state. The (red) dotted curve is the best-fit $n = 1$ parameter basic spectral equation of state, the (green) dashed curve is the best-fit $n = 2$ curve, and the (blue) dot-dash curve is the best-fit $n = 3$ curve.

spectral parameters $\{\gamma_0, \gamma_1, \ldots, \gamma_{n-1}\}$ in an n-parameter fit, simply set

$$\gamma_0 = \log\Gamma_0, \tag{7}$$

where Γ_0 is defined in Eq. (6), and then adjust the n spectral coefficients $\{\gamma_1, \gamma_2, \ldots, \gamma_n\}$ instead. Figure 2 illustrates the resulting best-fit representations of the APR1 equation of state in the neighborhood of the matching point (p_0, ϵ_0). Comparing the improved representations in Fig. 2 with the basic representations in Fig. 1 shows that this simple change is effective in removing the unphysical slope discontinuities at the match point.

The accuracy and efficiency of these improved basic spectral representations have been tested by computing best-fit models of the 27 (causal) theoretical neutron-star equations of state described in [2]. Figure 3 illustrates the averages of these fitting errors over the set of test equations of state for the $n = 1, \ldots, 5$ basic and improved basic spectral representations. The average errors plotted here are evaluated by computing a rms model error by summing the squares of the differences at the tabulated points of the exact equation of state in the relevant density range, and then averaging those averages over the collection of 27 equations of state used in this study. This type of average error was introduced and used in [2]. These results show that the improved basic spectral representations, in addition

[1]The APR1 equation of state was chosen as a representative because its spectral fits have errors that are close to the averages of the errors for the model equations of state studied in [1].

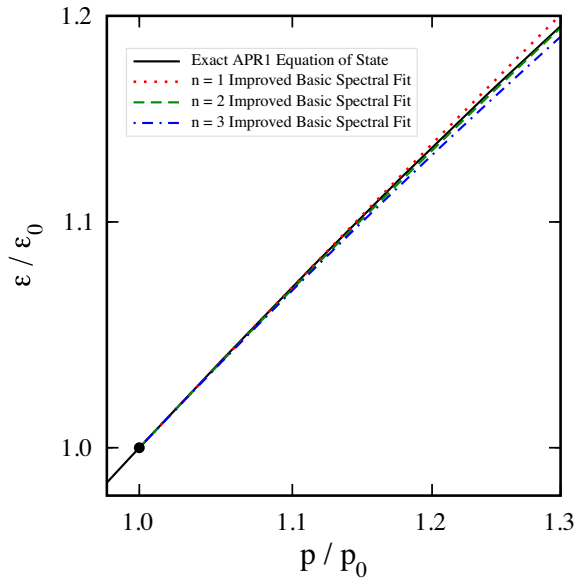

FIG. 2. Continuity and differentiability of the improved pressure-based basic spectral representations are illustrated at the point (p_0, ϵ_0) (black dot) where the best-fit spectral equations of state match onto the low-density equation of state. The exact equation of state shown here as the solid (black) curve is the APR1 equation of state. The (red) dotted curve is the best-fit $n = 1$ parameter improved basic spectral equation of state, the (green) dashed curve is the best-fit $n = 2$ curve, and the (blue) dot-dash curve is the best-fit $n = 3$ curve.

to removing the unphysical phase transition discontinuities at the matching point, are also somewhat more accurate on average than the basic spectral representations with the same number of adjustable parameters. The 27 exact equations of state used for these tests include several that have phase transitions within the density range covered by these spectral fits. Those equations of state are included in the average errors displayed in Fig. 3. Their errors are somewhat larger (typically a few times larger) than the averages shown here for these low-order representations with $n \leq 5$. More detailed information about the errors associated with each of the exact equations of state included in this study can be found in [1,2].

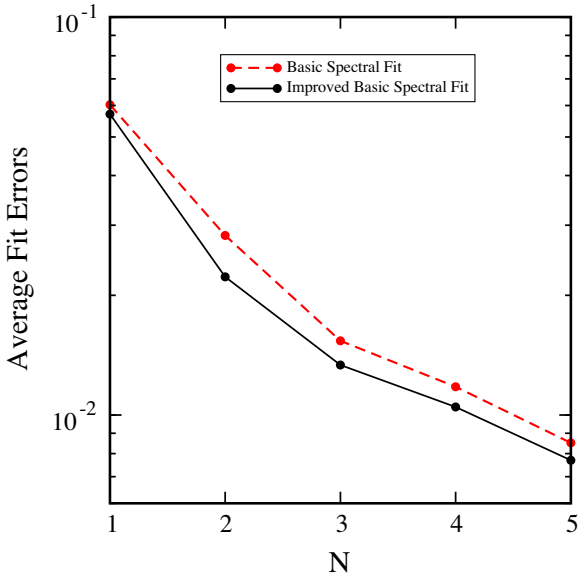

FIG. 3. Average errors of the n-parameter pressure-based basic and improved basic spectral fits are illustrated for 27 realistic neutron-star equations of state.

III. CAUSAL SPECTRAL REPRESENTATIONS

Spectral representations of the equation of state have also been developed that ensure causality [2]. These causal representations are faithful in the sense that every causal equation of state can be represented in this way, and every choice of spectral coefficients in these representations produces a causal equation of state. These causal representations are based on spectral expansions of the sound-speed function $\Upsilon(p)$, defined by

$$\Upsilon(p) = \frac{c^2 - v^2(p)}{v^2(p)}, \tag{8}$$

where $v(p)$ is the sound speed of the material,

$$v^2(p) = \left(\frac{d\epsilon(p)}{dp}\right)^{-1}, \tag{9}$$

and c is the speed of light. The sound speed must be less than the speed of light, $v(p) \leq c$, for any material that satisfies causality, so $\Upsilon(p) \geq 0$ for these materials.

The equation of state, $\epsilon = \epsilon(p)$, determines $\Upsilon(p)$ via Eqs. (8) and (9). Conversely, any $\Upsilon(p)$ on the domain $p \geq p_0$ determines the equation of state, $\epsilon(p)$, on that domain:

$$\epsilon(p) = \epsilon(p_0) + \frac{p - p_0}{c^2} + \frac{1}{c^2}\int_{p_0}^{p} \Upsilon(p')dp', \tag{10}$$

see Ref. [2]. Therefore any $\Upsilon(p) \geq 0$ determines a causal equation of state.

The causal spectral representations of the equation of state introduced in [2] were based on the following spectral expansions of $\Upsilon(p)$,

$$\Upsilon(p) = \exp\left[\sum_k \lambda_k \Phi_k(p)\right], \tag{11}$$

where $\Phi_k(p)$ are fixed spectral basis functions and λ_k are spectral coefficients. These spectral expansions determine an $\Upsilon(p)$ that satisfies $\Upsilon(p) \geq 0$, and therefore a causal equation of state. If the $\Phi_k(p)$ are a complete set of basis functions on a particular domain, then any $\Upsilon(p)$ can be represented in this way on that domain.

These causal representations were shown to be efficient and accurate ways to represent realistic neutron-star equations of state in [2]. In that study a collection of 27 different causal nuclear-theory based neutron-star equations of state were used to test the accuracy of these representations. Best-fit spectral expansions were prepared by adjusting the lowest-order spectral coefficients, $\{\lambda_0, \lambda_1, \ldots, \lambda_{n-1}\}$, to minimize the differences between the exact and the spectral representation of each equation of state. These spectral expansions were quite accurate, with average errors of 2%–3% for $n = 2$ representations and progressively smaller errors as the number of basis functions n is increased. The spectral representations had systematically smaller average errors than other popular piecewise-analytical representations with the same number of adjustable parameters. Therefore the spectral-based representations were found to be both accurate and efficient.

The spectral basis functions used in [2] for the causal representations were the same as those used for the basic representations in Eq. (5). It follows that the causal spectral representations have $\Upsilon(p_0) = \exp(\lambda_0)$ at the point (p_0, ϵ_0) where the high-density spectral representation matches onto the low-density equation of state. Therefore the sound speed at this point in the causal spectral representations is determined entirely by λ_0:

$$v^2(p_0) = \frac{c^2}{1 + \exp(\lambda_0)}. \tag{12}$$

The sound speed at this matching point can also be determined from the low-density equation of state in the usual way:

$$v_0^2 = \left(\frac{d\epsilon(p)}{dp}\bigg|_{p \uparrow p_0}\right)^{-1}. \tag{13}$$

It follows that the sound speed (and hence the derivative of the equation of state) will be continuous at this matching point if and only if $v(p_0) = v_0$. This agreement is possible if and only if the spectral parameter λ_0 has the value,

$$\lambda_0 = \log\left[\frac{c^2 - v_0^2}{v_0^2}\right]. \tag{14}$$

The n-parameter spectral representations described in [2] use the n lowest-order spectral parameters, $\{\lambda_0, \lambda_1, \ldots, \lambda_{n-1}\}$ to determine the equation of state. The best possible match between the exact nuclear-theory equations of state, and their spectral representations is achieved by adjusting the values of these n spectral parameters to minimize the differences. Similar to the basic spectral representations discussed in Sec. II, these optimal parameter choices typically produce λ_0 that do not satisfy Eq. (14) exactly. The graphs of the resulting best-fit causal spectral representations in the neighborhood of the matching point are similar to those shown in Fig. 1, so those graphs are not reproduced here. All the graphs show n-dependent discontinuities at the matching point with the low-density equation of state. There is, however, one qualitative difference between the causal graphs and those for the basic spectral representations: In the causal spectral representations the discontinuity in the slopes at the matching point are significantly larger for the $n = 1$ representations than that shown in Fig. 1.

The causal spectral representations can easily be improved, however, by setting λ_0 using Eq. (14) to ensure continuity of the sound speed at the matching point, and then adjusting the n parameters $\{\lambda_1, \lambda_2, \ldots, \lambda_n\}$ instead of $\{\lambda_0, \lambda_1, \ldots \lambda_{n-1}\}$. The accuracy and efficiency of these improved representations have been tested by comparing the best-fit models for the 27 (causal) model neutron-star equations of state described in [2]. Figure 4 illustrates the averages of these fitting errors over the set of test equations of state for the $n = 1, \ldots, 5$ causal and improved causal representations. These results show that the improved causal spectral representations, in addition to removing the unphysical phase transition discontinuities at the matching point, are also more accurate on average than the causal spectral representations with the same number of adjustable parameters. This improvement in accuracy is most pronounced for representations with small numbers of basis functions. The currently available data from neutron-star observations is not accurate enough or plentiful enough to allow very precise measurements of the equation of state. So having very accurate low-order representations should be particularly useful at this time.

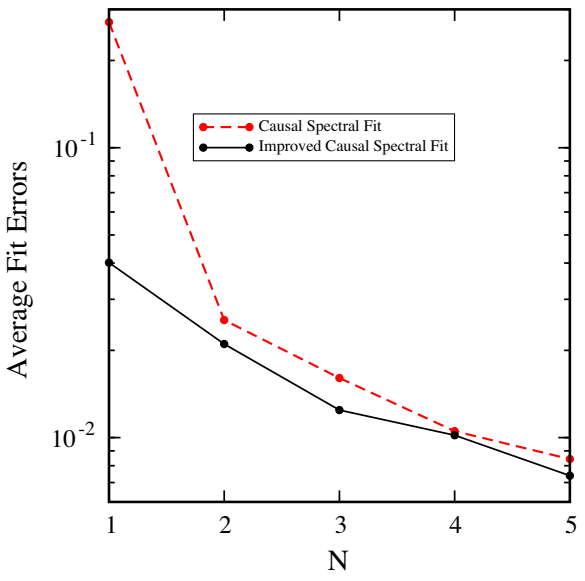

FIG. 4. Figure illustrates the average errors of the n-parameter pressure-based causal and the improved causal spectral fits to 27 realistic neutron-star equations of state.

IV. ENTHALPY-BASED REPRESENTATIONS

For some purposes it is more convenient to express the equation of state, $\epsilon = \epsilon(p)$, in terms of the enthalpy of the material, $h(p) = \int_0^p dp'/[\epsilon(p') + p']$, see e.g., Ref. [6]. The enthalpy version of the equation of state is generally expressed as the pair of functions $\epsilon = \epsilon(h)$ and $p = p(h)$. Basic spectral representations of these enthalpy-based equations of state have been given in [1] and causal representations in [2]. Like their pressure-based counterparts, the basic enthalpy-based representations are based on spectral expansions of the adiabatic index $\Gamma(h)$, which then determines the equation of state by quadratures (see Ref. [1]):

$$p(h) = p_0 \exp\left[\int_{h_0}^{h} \frac{e^{h'} dh'}{\tilde{\mu}(h')}\right], \tag{15}$$

$$\epsilon(h) = p(h)\frac{e^h - \tilde{\mu}(h)}{\tilde{\mu}(h)}, \tag{16}$$

where $\tilde{\mu}(h)$ is defined as,

$$\tilde{\mu}(h) = \frac{p_0 e^{h_0}}{\epsilon_0 + p_0} + \int_{h_0}^{h} \frac{\Gamma(h') - 1}{\Gamma(h')} e^{h'} dh'. \tag{17}$$

The constants p_0 and ϵ_0 are defined by $p_0 = p(h_0)$ and $\epsilon_0 = \epsilon(h_0)$ respectively.

Similarly the enthalpy-based causal representations are based on spectral expansions of the sound-speed function $\Upsilon(h)$, which also determines the equation of state by quadratures (see Ref. [2]):

$$p(h) = p_0 + (\epsilon_0 c^2 + p_0)\int_{h_0}^{h} \hat{\mu}(h') dh', \tag{18}$$

$$\epsilon(h) = -p(h)c^{-2} + (\epsilon_0 + p_0 c^{-2})\hat{\mu}(h), \tag{19}$$

where $\hat{\mu}(h)$ is defined as,

$$\hat{\mu}(h) = \exp\left\{\int_{h_0}^{h} [2 + \Upsilon(h')] dh'\right\}. \tag{20}$$

As in the pressure-based cases discussed in Secs. II and III, the continuity of the derivative of the equation of state at the matching point where $\epsilon_0 = \epsilon(h_0)$ and $p_0 = p(h_o)$ is determined by the continuity of $\Gamma(h_0)$ or $\Upsilon(h_0)$ at this point. The spectral basis functions $\Phi_k(h)$ used in the accuracy and efficiency studies in [1,2] are given by

$$\Phi_k(h) = \left[\log\left(\frac{h}{h_0}\right)\right]^k. \tag{21}$$

This basis has the property that $\Phi_0(h_0) = 1$ and $\Phi_k(h_0) = 0$ for $k > 0$. Therefore the expressions for $\Gamma(h_0) = \exp(\gamma_0)$ and $\Upsilon(h_0) = \exp(\lambda_0)$ at the matching point are identical to those for the pressure-based representations. Consequently the conditions needed to ensure the enthalpy-based spectral equations of state match the low-density equation of state with continuous derivatives are identical to those for the pressure-based representations: Eqs. (7) and (14) respectively.

The enthalpy-based spectral expansions can therefore be improved using the same method used for the pressure-based representations in Secs. II and III. Instead of

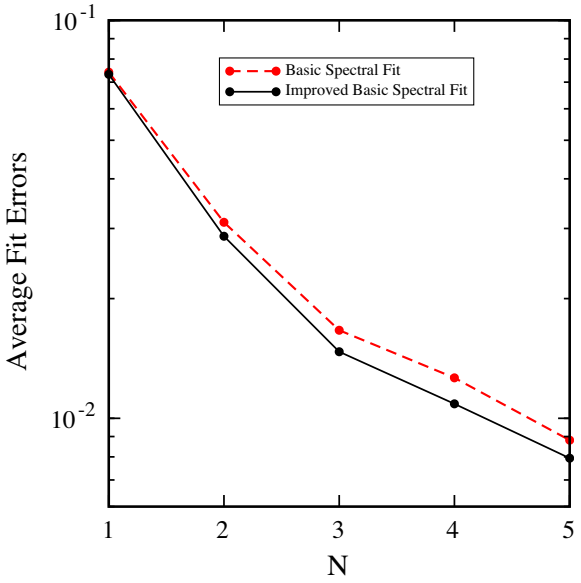

FIG. 5. Average errors of the n-parameter enthalpy-based basic and improved basic spectral fits are illustrated for 27 realistic neutron-star equations of state.

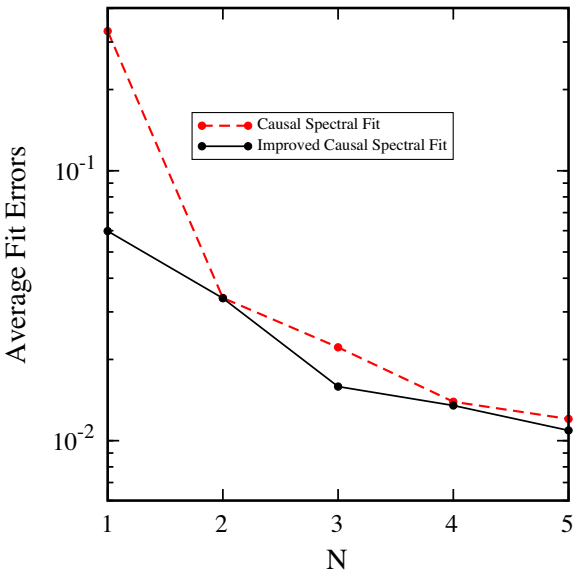

FIG. 6. Average errors of the n-parameter enthalpy-based causal and improved causal spectral fits are illustrated for 27 realistic neutron-star equations of state.

adjusting the parameters $\{\gamma_0,\gamma_1,\ldots,\gamma_{n-1}\}$ or $\{\lambda_0,\lambda_1,\ldots,\lambda_{n-1}\}$ to obtain the optimal n-parameter representations, the lowest-order parameters, γ_0 or λ_0, are fixed using Eqs. (7) or (14), while the n parameters $\{\gamma_1,\gamma_2,\ldots,\gamma_n\}$ or $\{\lambda_1,\lambda_2,\ldots,\lambda_n\}$ are adjusted for the best fits. The average errors in the best fits to 27 realistic neutron-star equations of state are illustrated in Fig. 5 for the basic and the improved basic enthalpy-based representations, and in Fig. 6 for the causal and the improved causal representations. As in the pressure-based representations, the accuracies of the improved enthalpy-based representations for a given value of n are systematically better than the original representations.

ACKNOWLEDGMENTS

This research was supported in part by NSF Grant No. 2012857 to the University of California at San Diego.

[1] L. Lindblom, Phys. Rev. D **82**, 103011 (2010).
[2] L. Lindblom, Phys. Rev. D **97**, 123019 (2018).
[3] B. P. Abbott, R. Abbott, T. Abbott, F. Acernese, K. Ackley, C. Adams, T. Adams, P. Addesso, R. X. Adhikari, V. B. Adya *et al.*, Phys. Rev. Lett. **121**, 161101 (2018).
[4] M. Miller, F. K. Lamb, A. Dittmann, S. Bogdanov, Z. Arzoumanian, K. C. Gendreau, S. Guillot, A. Harding, W. Ho, J. Lattimer *et al.*, Astrophys. J. Lett. **887**, L24 (2019).
[5] G. Raaijmakers, S. Greif, T. Riley, T. Hinderer, K. Hebeler, A. Schwenk, A. Watts, S. Nissanke, S. Guillot, J. Lattimer *et al.*, Astrophys. J. Lett. **893**, L21 (2020).
[6] L. Lindblom, Astrophys. J. **398**, 569 (1992).